REVIEW

Multidetector-row CT angiography in the study of atherosclerotic carotid arteries

Luca Saba · Roberto Sanfilippo · Raimondo Pirisi ·
Luigi Pascalis · Roberto Montisci · Giorgio Mallarini

Abstract Pathologies of the carotid arteries, and in particular atherosclerosis, are now an important medical problem. Stroke is the third leading cause of severe disability in the Western World leading to millions of deaths every year. Extracranial carotid atherosclerotic disease is the major risk factor for stroke. In years, with the advent of multidetector-row CT (MDCT) scanners and the use of specific angiographic protocols (MDCTA), CT imaging of the carotid arteries has become increasingly effective. In addition, the volume data obtained can be further rendered to generate high-quality two-dimensional and three-dimensional images. The purpose of this study was to review the atherosclerotic carotid arteries, their complications and how MDCTA depicts them, underlining the benefits and pitfalls of this diagnostic technique.

Keywords MDCTA · Carotid arteries

L. Saba (✉) · G. Mallarini
Department of Radiology, Policlinico Universitario,
s.s. 554 Monserrato,
09045 Cagliari, Italy
e-mail: lucasaba@tiscali.it

G. Mallarini
Institute of Radiology, Ospedale San Giovanni di Dio,
46 Hospital Street,
09126 Cagliari, Italy

R. Sanfilippo · R. Montisci
Department of Vascular Surgery, Policlinico Universitario,
s.s. 554 Monserrato (Cagliari),
09045 Cagliari, Italy

R. Pirisi
Division of Cardiology, Ospedale San Giovanni di Dio,
Cagliari 46 Hospital Street,
09126 Cagliari, Italy

L. Pascalis
Division of Internal Medicine, Ospedale San Giovanni di Dio,
Cagliari 46 Hospital Street,
09126 Cagliari, Italy

Background

Several types of pathologies may affect carotid arteries and among these atherosclerosis is a widespread medical problem. From the first study of Savory [1] in 1856 it has been known how atherosclerosis and stenosis of the carotid arteries may produce stroke. Currently this pathology is the third leading cause of severe disability in the Western World causing millions of deaths every year [2–4]. The pathogenesis of stroke is not yet completely understood although it may be briefly ascribed to two major process: (1) hypoperfusion from high degree of stenosis/occlusion of the vessel [5, 6], an (2) distal embolization [7, 8]. However, while it is likely that some strokes associated with carotid artery disease result from hypoperfusion, the majority of such events appear be the consequence of embolization of an atherosclerotic plaque or acute occlusion of the carotid artery with distal propagation of the thrombus.

In order to plan the best medical treatment it is important to identify all pathological signs in the carotid artery. In recent years, three studies—NASCET (North American Symptomatic Carotid Endarterectomy Trial), ECST (European Carotid Surgery Trial) and ACAS (Asymptomatic Carotid Athero-Sclerosis Group)—have provided cut-off values for the degree of stenosis indicating possible benefits of carotid endarterectomy (CEA) [9–11]. In particular the NASCET [9] proved the benefits of CEA in patients with symptomatic high-grade (70–99%) stenosis. Several recent studies, however, have provided evidence of the need to assess additional morpho-

logical parameters in order to better define the most correct therapeutic treatment. Most important are: plaque ulceration, the presence of a fissured fibrous cap, and the type of plaque (fatty, mixed or calcified) [12–15].

The concept of a "vulnerable plaque" [13] has been postulated for coronary arteries [16], but it may also be valid for carotid arteries. The so-called "vulnerable plaque" is an atherosclerotic plaque that contains a large necrotic lipid core covered by a thin or disrupted fibrous cap which is characterized by a high tendency to rupture, potentially resulting in embolization or thrombosis. Considering these characteristics we can state that even low-grade stenosis can result in a cerebrovascular event, so it is important to look beyond the lumen [17] to plaque morphology as well.

Isotropic voxels, high spatial and temporal resolution (not remotely comparable with conventional DSA for temporal resolution), the use of fast rate of injection of contrast material and postprocessing tools have improved the sensitivity and specificity of multidetector-row CT (MDCT) angiography (MDCTA) [18, 19]. Moreover, besides the degree of stenosis, MDCT clearly depicts the several layers which constitute the arterial wall. As a consequence, with the recent discovery of the importance of plaque vulnerability in the development of ischemic symptoms, considerable attention has been devoted to determining noninvasively plaque morphology. The aim of this paper is to review and to analyze the benefits and pitfalls of the use of MDCTA in the study of atherosclerotic carotid arteries and how MDCTA can assess them.

General technical parameters

MDCTA acquisition parameters including section thickness, increment, pitch, kV and mAs can markedly change according to the CT scanner employed and to the detector number. For this reason these aspects will be not specifically described in this work (Table 1). Usually, the first step in studying carotid arteries by MDCTA is the acquisition of a lateral scout image in order to define the correct field of view (FOV). The use of a reduced field of view results in an adequate spatial

resolution to detect even small alterations and limits the postprocessing procedures during the reformation phase. The FOV varies according to the neck morphology, but usually its range is between 12 an 18 cm. Patients have to lie supine, with the head tilted back to prevent dental artifacts on the images. They must also be instructed not to breathe and not to swallow. Some authors suggest performing a basal acquisition [20]. Detection of the exact position of the carotid bifurcation allows better definition of where acquisitions should be made. The angiographic phase then begins. Arterial enhancement is provided by the intravenous injection into an antecubital vein of 80–120 ml of nonionic iodinated contrast material [21, 22] at a variable rate from 3 to 6 ml/s. On the basis of hemodynamic and vascular anatomic data, in order to obtain an optimal image quality, injection of contrast material should be made into the right arm during deep inspiration [23]. This is because the right brachiocephalic vein runs parallel to the ascending aorta while the left brachiocephalic vein differs in course and length so that it could be compressed by the aortic arch posteriorly and sternum anteriorly.

The volume of contrast material depends upon the scan time which itself depends upon the number of detector rows of the scanner (4-s scan time in a 64-row scanner to cover 25 cm; Table 1). The acquisition delay time is individually determined for each patient using a bolus tracking system (Sure Start, Smart Prep, CARE bolus) or even using personal observation to empirically calculate the delay that usually ranges from 11 to 16 s. The contrast material bolus may be followed by a saline bolus in order to reduce streak artifacts due to beam hardening.

An antecubital vein is usually chosen, but other sites may be used, and if another site is used the delay time, which is the delay in seconds between the start of injection of contrast material and MDCTA acquisition, should be calculated again. Window level and window center are generally set at 700 HU and 200 HU respectively. Clave et al. [24], in a study using phantoms, found that a luminal attenuation of 150 HU is optimal for accurate assessment of carotid stenosis. A luminal attenuation <100 HU or >250 HU may reduce the accuracy. Usually optimal luminal attenuation of 150 HU is obtained using a flow rate of 3 ml/s. However, in our institute, high flow rates are routinely employed (3–6 ml/s) and we have observed optimal results even with 300–400 HU of luminal opacification.

General abilities and limitations of MDCT scanners

In this section we discuss the general abilities and limitations of modern MDCT, in particular the speed of the examination, the quality of the images, and the ability to view the data in two-dimensional (2-D) and three-

Table 1 MDCTA acquisition parameters

No. of detectors	Volume of contrast material (ml)	Flow rate (ml/s)	Section thickness (mm)	Pitch	Rotation time (s)	Scan time (s)[a]
4	120	6	1	1.5	0.5	21
16	100	5	0.75	1.5	0.5	7
64	80	5	0.6	1.3	0.33	4

[a] For a 25-cm length

dimensional (3-D) modes. The latest generation of MDCT scanners have a variety of benefits and new applications. MDCT scanners are markedly faster than spiral or sequential CT scanners.

CT angiography (CTA) has been significantly improved with the introduction of 64-section spiral CT scanners which enable rapid acquisitions of an isotropic dataset [25]. Since the introduction of 16-detector row scanners, the routine acquisition of volumes with isotropic submillimeter spatial resolution has been possible with scan times of less than 10 s for a coverage of 300 mm [26]; for example, CTA of the carotid arteries and the circle of Willis with 16 sections at 0.75 mm collimation, a rotation time of 0.5 s and a pitch of 1.5 requires only 9 s for a scan range of 250 mm (with a table feed of 36 mm/s). Scanners with 64 or more detector rows offer even better performances: gantry rotation times are decreased to 0.33 s, and section widths of 0.5 mm are available. So, examination of the whole length of the carotid arteries from the aortic arch to the circle of Willis (a scan range of approximately 250 mm) requires only 4 s with a 64-detector row CT scanner (64×0.6 mm, pitch 1.33, rotation time 0.33 s).

Faster acquisitions provide a better image quality since artifacts (respiration, swallowing, pulsation of the aorta, short arteriovenous circulation) are reduced. MDCT can provide a lower level of artifacts than single-row helical CT with a faster table speed. In this way it is possible to acquire true arterial phase imaging of the entire carotid artery with high spatial resolution [27] in less time. Axial spatial resolution may reach 0.3 mm; this value is determined by detector geometry and convolution kernel . An increased detectors number does not provide better in-plane spatial resolution, whereas z resolution is dramatically improved by increasing the number of detectors.

Image visualization and analysis tool

In the evaluation of carotid arteries the first-line study is the analysis of axial images, where it is extremely important to use both a correct window level and a correct window width. Values in several previous studies vary markedly [28–30], but typical set values are 700 HU and 200 HU for the window width and window level, respectively: these values commonly allow the lumen with contrast material from the arterial wall (in particular in the presence of calcified plaque [31]) to be separated. However, there are a range of values and the choice of values depends on the situation. Choosing the wrong values may significantly alter the visualization of the lumen and consequently affect the estimate of stenosis percentage.

The attenuation in Hounsfield units may be measured using a circular or elliptical region of interest cursor in the predominant plaque area at each level.

Several reformatting techniques are available for assessing the carotid arteries: maximum intensity projection (MIP), multiplanar reconstruction (MPR), curved planar reconstruction (CPR) and volume rendering (VR). All these techniques show strengths and pitfalls since they are based upon different procedures for postprocessing the CT data.

In MIP, only the voxel with highest CT number is displayed depending on the voxel position along the projecting ray [32]. MIP may generate high-quality DSA-like images (Fig. 1) providing an overview of the target vessel. On the other hand, it shows a lower sensitivity in the presence of dense calcification or indwelling stents since it may obscure contrast material in the lumen. Generally, MIP is preferred to MPR because MIP reformations project only pixels with the highest attenuation, whereas MPR averages the attenuation of the pixels along the axis of projection.
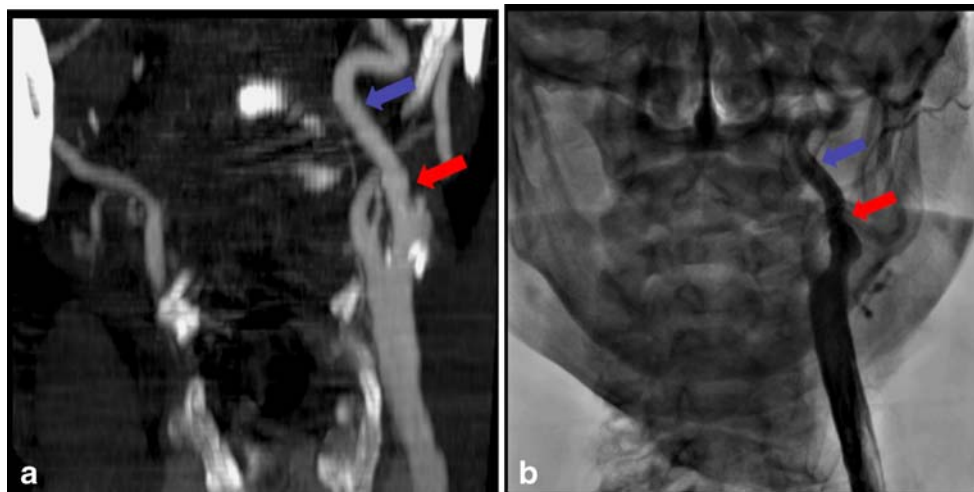

Fig. 1 A 63-year-old man. MIP reconstructed image (**a**) and DSA image (**b**). Stenosis of the left internal carotid artery (*blue arrows*). The lumen filled with contrast material is visible in both images (*red arrows*)

Often, it is relevant to use (thin or thick) slab MIP [33] to limit the over-projection phenomenon, in order to avoid time consuming editing to exclude ebony structures.

MPR is perhaps the simplest and most commonly applied reformatting method [33]. MPR creates views in an arbitrary plane without loss of information [34, 35]. MPR involves the retrospective reconstruction of axial images and the image obtained may be oriented in any spatial direction (Fig. 2). Moreover, using a 32–64 slice scanner producing isotropic voxels, the spatial resolution is similar to that of the original source images. MPR images show great utility in quantitative lumen analysis and in axial image plane definition because they depict the shape of the lumen.

CPR is a 2-D image that shows the cross-sectional profile of a vessel along its length (Fig. 3) preserving the relative x-ray attenuation [36–38]. An important issue concerning the use of the CPR is that the vascular images depend on the course of the selected curved plane. If the operator selects an inexact plane, it will generate an erroneous morphology and degree of stenosis. We think that CPR is not accurate in stenosis measurement and should not be used at all for this purpose.

VR is an advanced computer rendering algorithm [39]. It incorporates all the raw CT data to produce a high-quality 3-D image (Fig. 4). Since the layout of the lumen can change according to the threshold value, this reconstruction technique may produce errors in the dimensional evaluation
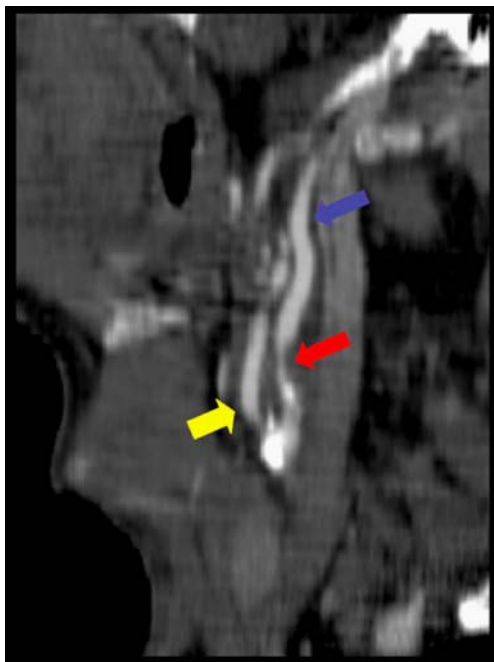
Fig. 2 A 79-year-old man with a transient ischemic attack. MPR image. Severe stenosis of the right carotid bulb is clearly visible (*red arrow*) (*blue arrow* internal carotid artery, *yellow arrow* external carotid artery)
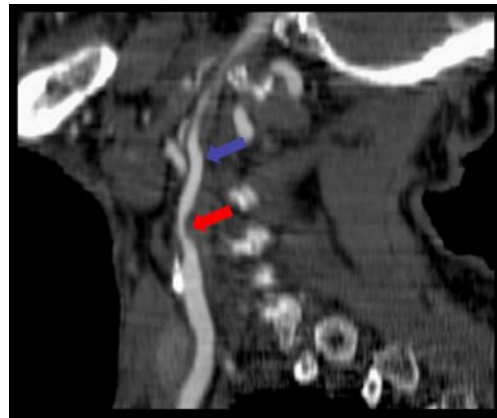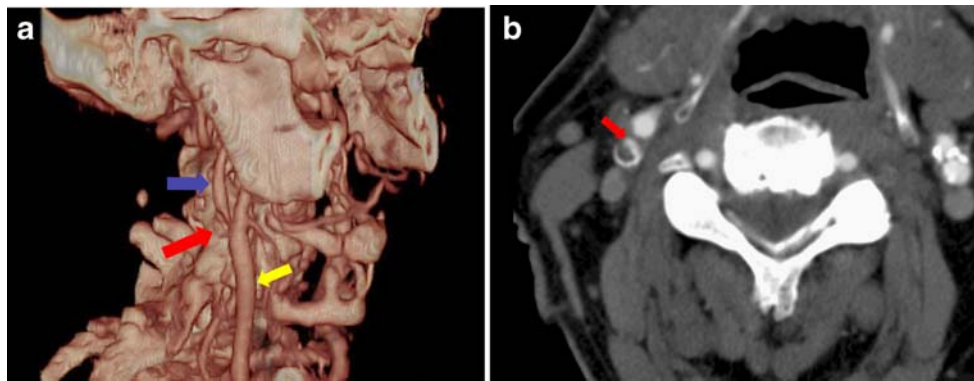

Fig. 3 A 79-year-old man with a transient ischemic attack. CPR image, the same patient as in Fig. 2. Severe stenosis of the right carotid bulb is clearly visible (red arrow) (*blue arrow* internal carotid artery)

of the degree of stenosis. Advanced VR algorithms enable mural calcifications to be distinguished from the residual lumen [28], and this algorithm is very useful for detecting ulcerated carotid plaques [18].

How to define the degree of stenosis and the problem of near-occlusion

The degree of stenosis is currently the leading parameter in choosing the therapeutic option. NASCET and ECTS investigators evaluated the degree of stenosis as the percentage reduction in the linear diameter of the artery. Differences exist in the evaluation of the degree of stenosis between NASCET and ECST (Table 2 and Fig. 5) and values derived from these two classification methods for the same carotid stenosis are not equal, so it is always important to specify the classification used. In both NASCET and ECST, to quantify the degree of stenosis [40], measurements have to be performed strictly perpendicular to the carotid axis. Moreover, for almost a decade workstations available have been capable of producing high-quality 2-D and 3-D postprocessed images [34]. We can state that the sensitivity of MDCTA in evaluating the degree of stenosis may be comparable to that of angiography but with a lower level of risk [20, 41–51]. In particular, CTA, with sensitivities between 70% and 99% for stenoses of the internal carotid artery (ICA), with angiography as the reference standard, can provide excellent results [43–50].

Using axial images for the estimation of the degree of stenosis (Fig. 6) allows exact differentiation of the residual lumen from pathological plaque. Sometimes it may be difficult to adequately evaluate the degree of stenosis using axial images, in particular when carotid artery has acquired anomalies in its course. If kinking or coiling is present, it becomes mandatory to use reformatting tools in order to

Fig. 4 A 74-year-old man with stroke. VR image (**a**) and CTA axial source image (**b**). Severe stenosis of the right carotid bulb is clearly visible (*red arrow*) (*blue arrow* internal carotid artery, *yellow arrow* CCA). The high-grade stenosis is correctly depicted on the VR image (**a**) and is confirmed on the axial image (**b**)

assess the spatial course of the carotid artery and to correctly identify and measure the stenosis. In these situations the use of reformatting procedures is very important to exactly define the plane of the axial images and to ensure that all axial measurements are in a true perpendicular cross-sectional plane [52].

Large calcified plaques preclude MIP evaluation because of superimposition between the calcification and the contrast enhanced lumen. Moreover, heavy calcifications on both sides of the lumen can lead to overestimation of the stenosis in CT images because of the so-called "blooming" artifact [53]. The VR algorithm provides better results because of its capacity to distinguish calcifications from the contrast-enhanced residual lumen (Fig. 7).

In the evaluation of the carotid arteries, besides selecting a correct spatial position (strictly perpendicular to the carotid axis), the radiologist has to use both a correct window level and a correct window width. Choosing wrong values may significantly alter the visualization of the lumen and consequently modify the estimated stenosis percentage.

MDCTA may also be an adequate alternative to catheter angiography in the diagnosis of internal carotid near-occlusion versus total occlusion [54, 55]. Near-occlusion stenosis indicates a severe carotid bulb stenosis with a subsequent subtle decrease in size of the distal ICA lumen. Detection and precise interpretation of near-occlusion are important in arriving at a proper diagnosis and planning

treatment. Actually this circumstance cannot be considered as a surgical emergency because of the lower risk correlated with ipsilateral stroke. It has been also demonstrated that CEA/revascularization are less effective in these patients [6, 56–58]. The presence of near-occlusion affects the therapeutic approach to the pathological carotid artery. Fox et al. [6], using angiography, determined the following criteria to define the presence of near-occlusion: (1) the presence of notable stenosis of the ICA bulb, and (2) a reduction in the caliber of the distal ICA in comparison to (a) its expected lumen size, (b) the lumen size of the contralateral ICA, and (c) the lumen size of the ipsilateral external carotid artery (ECA). When the lumen of the distal ICA has partially collapsed it is possible to recognize the so-called "string sign". Bartlett et al. [54] have suggested, following the use
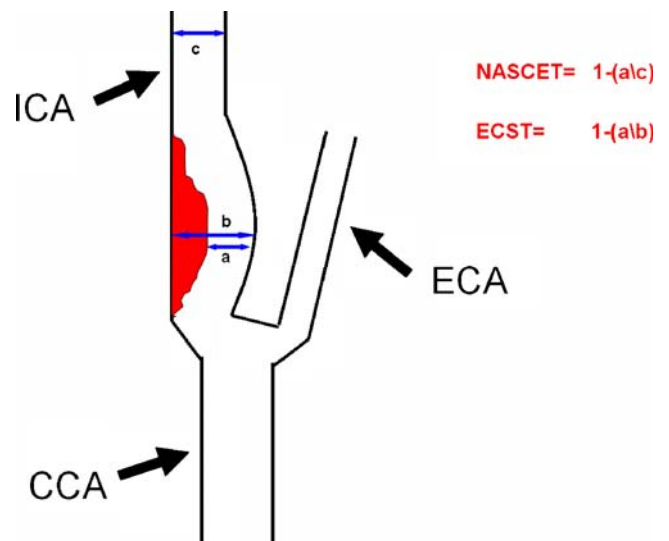
Fig. 5 Schematic drawing showing how to determine the percentage stenosis using NASCET and ECST criteria. With the NASCET criteria the ratio between the residual luminal diameter at the stenosis and the diameter of the distal normal lumen where there is no stenosis is calculated. With the ECST criteria the ratio between the residual luminal diameter at the stenosis and the total diameter is calculated

Table 2 Degrees of stenosis of the carotid artery as determined by the NASCET and ECST criteria

NASCET (%)	ECST (%)
30 to 69	50 to 82
52 to 99	70 to 99
70 to 99	82 to 99
50	75
60	80
70	85
80	91
90	97
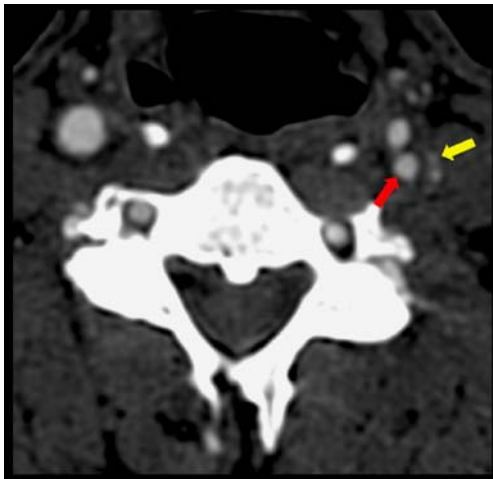
Fig. 6 A 65-year-old woman. Axial CTA source image. Stenosis of the left internal carotid artery. The residual lumen is visible (*red arrow*) together with an eccentric calcified plaque (*yellow arrow*)

of MDCTA, other methods to correctly identify near-occlusion including, in particular, a comparison of the distal ICA with the contralateral distal ICA. The authors suggest that the distal ICA ratio threshold value that best predicts near-occlusion stenosis with the greatest sensitivity and specificity is 0.87. This is a very effective criterion (sensitivity 97.3% and negative predictive value 99.4%), although it is important to remember that this method is not valid in the presence of disease of the contralateral ICA. The sensitivity of CTA in detecting near-occlusion stenosis is very high and is comparable to that of DSA, as reported by Chen et al. [59].

In the evaluation of carotid artery stenosis MR angiography (MRA) and duplex ultrasound (DUS), as well as CTA, are widely used. DUS is commonly performed to screen patients with possible carotid artery disease, but the accuracy of sonography is moderate in assessing the degree of stenosis [60]. The use of DUS as the only diagnostic test

Fig. 7 A 77-year-old man with a transient ischemic accident (same patient as in Fig. 10). VR image. A large calcification (*red arrows*) is clearly visible in the bifurcation (*blue arrow* internal carotid artery, *yellow arrow* external carotid artery)

for selection of patients for CEA has been widely discussed [61–64]. If only DUS is used several critical errors can occur [60], and the number of false-negative findings of >70% stenosis can be very high [60]. Eliasziw et al. [60] and Collins et al. [65] have suggested that sonography should be used only as a screening tool to exclude patients with no carotid artery disease from further testing. In fact this technique has several limitations such as the variability in optimal thresholds and the limited amount of morphological information obtained [66], and moreover, the performance of DUS is highly variable. The use of color-flow Doppler US can increase accuracy, in particular, in differentiating near-occlusion from occlusion. In a study comparing CTA and DUS with conventional angiography as the reference [45], CTA was found to yield higher sensitivity, specificity and predictive values than DUS in assessing high-grade stenosis and distinguishing it from complete occlusion.

MRA is quite good at determining the degree of stenosis degree. In a wide series of studies that took carotid angiography as the gold standard, the median sensitivity for a high-grade lesion was 93%, whereas the median specificity was 88% [67]. MRA of the carotid artery may be accomplished by several different MRI techniques including 2-D TOF, 3-D TOF and contrast-enhanced MR angiography [68–71]. 2-D TOF provides a strong vascular signal, even when the rate of arterial blood flow is low. This technique allows correct differentiation of near and complete ICA occlusion. 3-D TOF provides superior resolution, but its sensitivity in measuring flow is lower than that of 2-D TOF. Contrast-enhanced MR angiography is a very promising technique that is not impaired by slow-flow situations. An important problem with MRA is the high variability between observers [72]. Lumen measurement can be inaccurate on source images and even in MRA as in CTA, the postprocessing of the images can influence the assessment [73].

Some authors [66, 74] have reported that both DUS and MRA tend to overestimate the degree of stenosis whereas CTA underestimates it. In a study by Marks et al. [43] comparing CTA and MRA, standard conventional CTA was found to be superior to MRA in the estimation of severe carotid stenosis and occlusion, although good results have recently been reported with MRI at 3 T [75].

Plaque morphology

Direct visualization and definition of plaques may lead to a better understanding of the natural history of atherosclerotic plaque [76], which has relevance in determining the most appropriate therapeutic plan. The definition of a plaque's composition and morphology is important because it is a

fundamental predictor of plaque stability. In addition the risk of plaque rupture may be correlated more with specific plaque composition than plaque volume [77, 78].

Using MDCTA it is possible to divide atherosclerotic plaques into three major types, determining plaque density in Hounsfield units: soft plaques, intermediate plaques, and calcified plaques. As we have previously reported, the attenuation in Hounsfield units may be measured using a circular or elliptical region of interest cursor in the predominant plaque area at each level. In recent studies [79, 80] using MDCTA, plaque has been characterized as fibrous tissue, lipid and calcifications, and these studies also provided a comparison with histology. The authors demonstrated that MDCT is able to quantify the total plaque area, calcifications, and fibrous tissue in good correlation with histology.

Soft plaques have density values <50 HU [81] (Fig. 8).

Most ruptures occur in fatty plaques, which contain a soft, lipid-rich core covered by a thin and inflamed cap of fibrous tissue. The concept of the "vulnerable plaque" that was first adopted to describe coronary arteries [13, 16], may be also used for carotid arteries. The term "vulnerable plaque" refers to an atherosclerotic plaque that contains a large necrotic lipid core covered by a thin or disrupted fibrous cap characterized by a higher tendency to rupture resulting in embolization or thrombosis. It has been demonstrated that the presence of a fatty plaque with a lipid core is significantly associated with the presence of cerebral infarction on MR brain imaging (P=0.03 [14]). It is also important to consider that even low-grade stenosis can result in cerebrovascular events so that it becomes of fundamental importance to look beyond the lumen [82], assessing both plaque type and morphology.
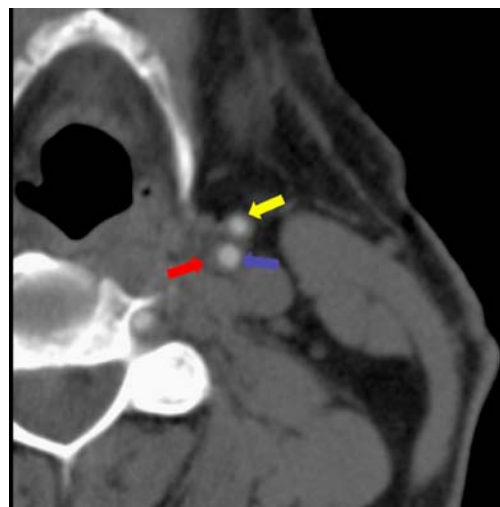
The attenuation of a selected area of a plaque can be readily quantified in Hounsfield units using CTA allowing classification as fatty or not. However, so far the fibrous cap and its potential rupture has been better visualized using MRI [83–86].

An extensive literature describes the potential of MRI in assessing carotid artery plaque morphology [87–91]. MRI is particularly attractive because it is noninvasive and it provides a rich array of information on vascular disease. In particular, the percentage of lipid-rich necrotic core can be quantified using high-R [87] and contrast-enhanced MRA [88]. Moreover, MR methods have been demonstrated to provide information on important features of vascular disease, such as the composition of atheroma.

More recently these tools have been used to detect the presence and activity of specific molecules that are fundamental participants in the inflammatory processes that are thought to influence the differentiation of stable plaque from vulnerable plaque.

On CTA, intermediate plaques show a density ranging from 50 to 119 HU (Fig. 9). Lesions with a density of >120 HU correlate with calcified plaque (Fig. 10). It has been suggested [15, 92] that calcified carotid atherosclerotic plaques causing stenosis are less likely to be symptomatic than noncalcified plaques, suggesting that calcifications confer stability. Calcium provides stability to the plaque, producing a protection against biomechanical stress and subsequent disruption.

Referring to reconstruction modalities, currently the most efficient visualization technique to study plaque components is the axial scan, which allows visualization of all the components showing their exact quantification.

Fig. 8 A 72-year-old woman with dysarthria. Axial CT image. In the left internal carotid artery (*blue arrow*) is visible fatty plaque (*red arrow*) that has produced type IV NASCET stenosis (*yellow arrow* external carotid artery). The mean density value in the fatty plaque was 38 HU (SD 14 HU)

Fig. 9 A 65-year-old woman. Axial CT image. In the left internal carotid artery (*blue arrow*) a mixed plaque (*red arrow*) is visible that has produced type III NASCET stenosis (*yellow arrow* external carotid artery). Mean density value in the mixed plaque was 68 HU (SD 23 HU)
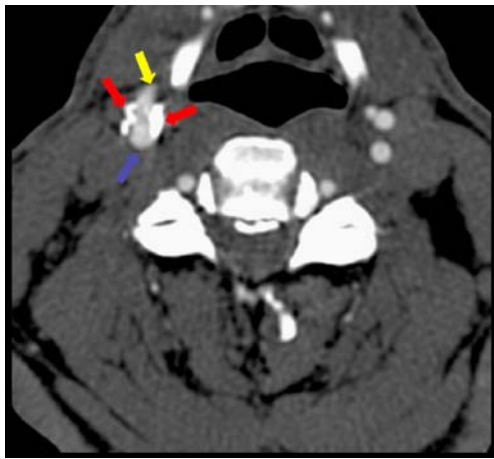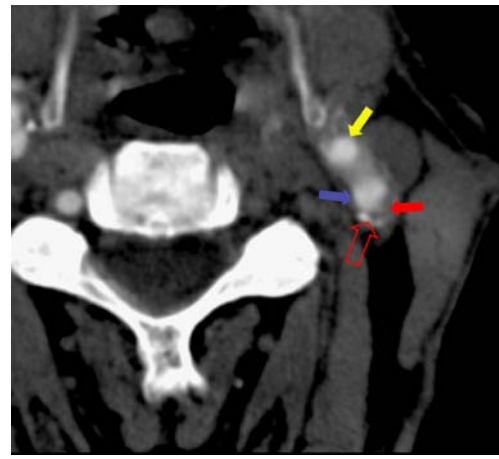
Fig. 10 A 77-year-old man with TIA (same patient as in Fig. 7). Axial CTA source image. In the bifurcation site complex calcified plaque (*red arrows*) is visible (*blue arrow* internal carotid artery, *yellow arrow* external carotid artery). Mean density value in the calcified plaque was 785 HU (SD 93 HU)

Fig. 11 A 71-year-old woman. Axial CT image. In the left internal carotid artery a complex mixed plaque with peripheral wall calcification (*red open arrow*) is visible (*red arrow* fissured fibrous cap, *blue arrow* internal carotid artery, *yellow arrow* external carotid artery)

The use of MIP cannot be recommended for the evaluation of plaque morphology because this algorithm only visualizes voxels with the highest number along a projection axis, losing all other components and providing partial and incomplete information. MPR, VR and CPR may be adequate (Fig. 7). In the assessment of calcified plaques, it is possible to use nonenhanced images because calcified components are highly visible and easily distinguishable from other carotid components without superimposition or artifacts derived from contrast medium. The use of precontrast scans is debatable, since calcifications are most often quite visible even with injection of iodine into the vessels. In the evaluation of plaque type and morphology, MDCTA shows benefits compared to angiography, that cannot provide adequate and exhaustive information in this application.

Ulcers, fissured fibrous cap, intraplaque hemorrhage and thrombosis

The presence of ulcers, a fissured fibrous cap, intraplaque hemorrhage and thrombosis may represent an increased risk of stroke [9], and their presence could affect the choice of treatment which could move from medical treatment to CEA or interventional therapy.

Some authors have noted that a ruptured or thin fibrous cap is an important feature in a vulnerable coronary artery. We have recently confirmed that a fibrous cap is an important indicator of vulnerability in the carotid artery as well [93, 94]. A fissured fibrous cap (Fig. 11) is the first predictive sign of fibrous cap rupture with consequent exposure of the thrombogenic component of the lipid nucleus. This is very difficult to detect using MDCT

because of its spatial resolution (a thin cap is about 65 μm thick). Concerning contrast resolution, moreover, to our knowledge there is only one report in the literature on this subject using MDCTA [94]. Studies have shown that MRI can sufficiently characterize a fibrous cap [93, 95–97].

Intraplaque hemorrhage is commonly observed in atherosclerotic plaques, and some authors believe that it may be due to rupture of the plaque neovasculature [98]. Intraplaque hemorrhages (Fig. 12) may be a marker of plaque instability which is a contributing factor to a more rapid progression of atherosclerosis. Hemorrhages are more common when a stenosis with a diameter reduction exceeding 70% is present [99]. In MDCTA images it is possible to visualize intraplaque hemorrhage as a region showing evidence of reduced contrast material passage.
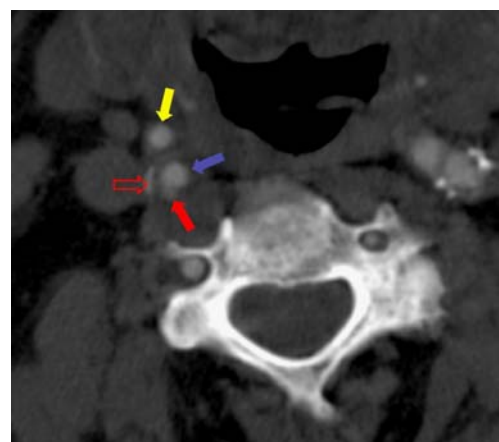

Fig. 12 A 73-year-old man. Axial CT image. In the right internal carotid artery a complex mixed plaque with peripheral wall calcification (*red open arrow*) is visible (*red arrow* intraplaque hemorrhage, *blue arrow* internal carotid artery, *yellow arrow* external carotid artery)

In axial images intraplaque hemorrhage is easily visible, and when its dimensions exceed 1 mm it is possible to visualize it using the various image reformatting techniques. However, on the basis of current data and indications in the literature, we believe that it is not possible to correctly detect intraplaque hemorrhage with CT [100, 101]. It is possible to distinguish a region with hypodensity (as described by Oliver et al. [100]) but there is no method by which the lipid necrotic and hemorrhagic components can be confidently differentiated. Moreover the association between symptoms and hemorrhage remains a controversial subject. Saam et al. [93] reported that 91% of patients with symptomatic plaques and 83% of patients of asymptomatic plaques had intraplaque hemorrhage (P=0.5). The authors suggested that the key point is not the presence or absence of hemorrhage, but whether the hemorrhage is acute (fresh/acute hemorrhages were significantly more likely to be found in patients with symptomatic plaques than in patients with asymptomatic plaques, P=0.021). This is an advantage of MRI because it can easily depict intraplaque hemorrhage and it offers the possibility of distinguishing between acute and nonacute hemorrhage.

Carotid ulceration is the third type of complication that we discuss here. The importance of plaque ulceration has been underlined in NASCET [9], where it was seen that ulcerated carotid plaques were responsible for 30% of ischemic cerebral events after 2 years in the group receiving medical therapy in comparison to 17% of events in subjects with no ulcerated plaques. So the presence of ulceration is an important risk factor for the stroke. We can define ulceration as a zone where some tissue is lost and contrast medium will appear in the axial scans as an "in plus" image (Fig. 13). In the study of ulcerated plaque angiography is not sufficiently reliable [102, 103] whereas MDCTA appears to offer good results in detecting ulcers in carotid artery plaques [104]. In particular with the use of postprocessing procedures it is possible to correctly identify and define the ulcer [18] (Fig. 14). Detecting ulcers can be difficult occur if plaques are calcified. In this situation correct characterization may be difficult. Some authors state that the presence of calcified plaques could limit the use of CTA [41, 42].

In our experience, the presence of an ulcerated carotid plaque may lead to difficulties in the differential diagnosis with carotid wall dissection on axial scans. This is because on axial images ulcer morphology may appear similar to dissection morphology. To solve this differential diagnostic issue, in most cases the use of VR may be sufficient, because it precisely depicts the spatial morphology of vessels allowing the communication between the ulcer and the carotid lumen to be visualized [18]. CTA is considered to be far superior to echo-color Doppler US in detecting ulcerations. Saba et al. [104] have reported the sensitivity of
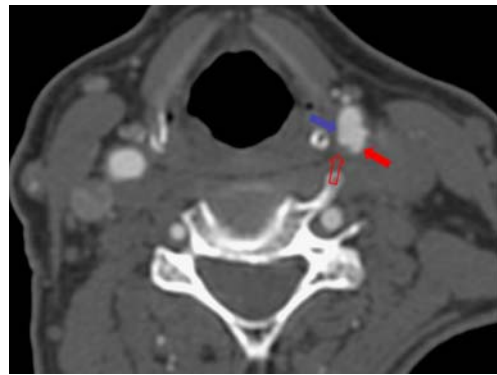

Fig. 13 A 71-year-old woman with persistent monocular visual loss. Axial CT source image. In the bifurcation (*blue arrow*) a mixed plaque (*red open arrow*) and an ulceration (*red arrow*) are visible. Ulceration was confirmed surgically

echo-color Doppler US in detecting ulcers to be only 37.5%. This value is similar to values reported by other authors [105–107]. MRI is effective in detecting plaque ulcerations [108].

Dissection of the carotid arteries is an important cause of stroke, accounting for up to 20% of ischemic strokes in young adults [109]. CTA has been found to provide results that closely agree with those obtained with angiography [110]. Criteria for diagnosis are considered to be the presence of a narrowed eccentric lumen in association with mural thickening and enlargement of the overall diameter of the ICA.

Surface thrombus was visible in nearly 30% of patients with ulcerated plaque reported by Rothwell et al. [111] in their angiographic/pathologic analysis of 1,671 patients. Thrombus may be found in complicated plaques and unstable plaques, and may lead to distal embolization. It is easily detected by CTA.
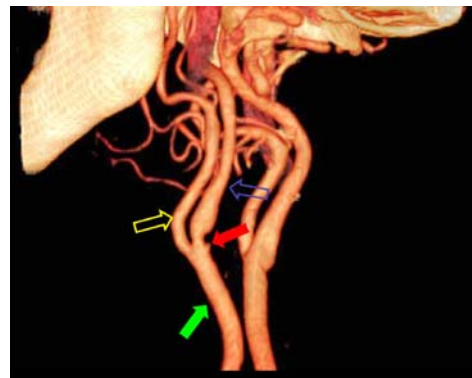
Fig. 14 VR image in the same patient as in Fig. 13. The ulceration (*red arrow*) is clearly visible in the bifurcation (*blue open arrow* internal carotid artery, *yellow open arrow* external carotid artery, *green arrow* common carotid artery)

Position of the plaque

A genetic predisposition is frequently seen in those with atherosclerosis and there are multiple risk factors such as hyperlipidemia, hypertension, smoking, diabetes mellitus, social stress, sedentary lifestyle and viral infection. However, despite its systemic nature it is a geometrically focal disease that has a propensity to involve the outer edges of blood vessel bifurcations [112]. An atherosclerotic plaque typically develops around the region of the internal and common carotid artery (Figs. 1, 6 and 10) and the internal carotid artery bulb is a predilection site for atheroma [10, 113, 114]. This led to wide acceptance of the hypothesis that hemodynamic forces play an important role in the development and progression of atherosclerosis.

The anatomic configuration of the carotid bifurcation, including the angle of the origin of the ICA, may be an important risk factor for carotid atherosclerosis [115]. Previous studies have shown that there is a sex difference in the distribution of carotid plaque [116]. Men are more likely to have the point of maximum stenosis distal to the bulb of the ICA, whereas women are more likely to develop disease of the ECA. These differences may be a consequence of the difference in bifurcation anatomy. A problem about the plaque position is whether atherosclerosis of the human carotid arteries is a bilaterally symmetrical disease or not. Adams et al. [117] have suggested that atherosclerosis is a bilaterally symmetrical disease, but other authors have suggested that the plaques in the same subject do not involve both carotid arteries to the same extent [118]. MDCTA, by integrating axial CT scans and reformatting procedures, is able to clearly depict both carotid arteries allowing correct evaluation of the position and geometry of the plaque. In particular, MIP and VR provide images with high spatial quality with information about the type, relationship and position of the plaques.

Tandem lesions

We speak of "tandem lesions" when there are two pathological stenoses in the same carotid space (Fig. 15): one is located in the carotid bifurcation and the other is located generally whether in the common carotid artery or in the arterial siphon. The incidence is nearly 10%. The presence of tandem carotid stenoses is thought by some authors to be a relative contraindication to CEA. Tandem stenoses have been viewed as a source of thrombus formation at the endarterectomy site because of the persistent slow flow through the stenosed segment. So it is important to detect and to characterize tandem lesions because the presence of this particular kind of stenosis may alter patients management [119]. Detection of tandem

Fig. 15 A 59-year-old woman. VR image. There are two calcified plaques, one in the bifurcation with continuation in the ICA (*red arrows*) and the second in the common carotid artery (*open red arrows*)

lesions is important because it allows the overall burden of disease within the carotid vessel to be defined prior to potential intervention (CEA, carotid stenting, medical treatment). Axial CTA may define disease, even very small plaques which may be missed on DSA or on reformatted CTA images. We have to add that sometimes the evaluation of the petrous segment of the carotid artery can be difficult because of the artifacts produced by bone structures [120].

Notes on radiation dose and reaction to contrast material

An important point that has to be considered is the risk of the MDCTA examinations. In particular, two distinct types of potential risk are possible: reaction to contrast material and radiation risk. Contrast material injection has a slight risk of causing an intolerance [121–125]. Reactions usually occur immediately and include flushing, itching or difficulty breathing or swallowing, but also nephropathy may be a serious consequence [126, 127]. An anaphylactic reaction requiring treatment can be expected in 1 to 500–5,000 injections. The risk is increased to 1 to 100–1,000 in patients with asthma, in patients with food and drug allergies, and in patients with a previous reaction to contrast material. The risk of death is 1 in 50,000 to 1 in 500,000 [122]. Overall iodine is safe and has been used for many years in millions of CT examinations. Iodine contrast increases the sensitivity of MDCTA examinations and it is

accepted worldwide that the benefits of using iodine contrast typically outweigh the risks. Moreover DSA, considered in recent years as the gold standard technique to study the carotid artery, shows a not negligible risk (2%) of complications after the procedure and the use of radiation is necessary [100, 128] (without considering the high cost).

Another important issue to be considered in performing a CT examination is the radiation dose. Exposure of the patient to radiation during CT examination and the consequent potential radiation hazard have recently received attention in both the scientific and general literature [129]. It is important to reduce radiation exposure. To obtain a reduction it is necessary to adjust the dose to the patient's weight and size [27]: a general rule for the radiologist is that the dose necessary to maintain constant image noise has to be doubled if the diameter of the patient increases by 4 cm, and obviously half the dose is sufficient for a patient with a diameter 4 cm smaller. So in a thick neck it is necessary to use a high kV, but in a thin neck using a reduced kV produces images of adequate quality in spite of the reduced dose. In a study by Ertl-Wagner et al. [130], with a tube current of 100 mAs and variable kV (80, 120 and 140), the mean effective doses were estimated to be 0.35, 0.99 and 1.37 mSv, respectively. The authors did not recommend the use 80 kV because of degradation of image quality, an increase in the photoelectric effect, and a decrease in Compton scattering.

In a study of the craniocervical vascular system [131], the mean effective radiation dose was found to be 2.31 ± 0.57 mSv . Using a 64-detector-row scanner the volume CT dose index should be less than 14 mGy/cm [132]. It is important to remember that additionally, the current 64-channel CT systems are equipped with an automatic exposure control system that continuously modulates the X-ray tube current based on patient size and tissue density [133, 134], and usually a reduction in radiation dose can be achieved. A dose reduction can also be achieved by omitting the basal scan and performing the CTA examination directly with contrast medium. In our experience a precontrast scans does not provide additional useful information and can be avoided. It is important to bear in mind that the radiation dose from DSA is higher than that from CTA: the dose from a 3-D DSA rotational acquisition is near 1,100 cGy cm^2 per acquisition.

Conclusion

MDCTA is a well-known important technique in the evaluation of atherosclerotic plaque and it may produce correct, precise and high-quality images. In our opinion, every patient in whom DUS has detected pathology should be evaluated with CTA, because the use of sonography alone does not produce acceptable results to inform the choice of therapeutic approach [60, 132]. The wide use of CT provides, in our opinion, optimal results and its sensitivity in the evaluation of the degree of stenosis is similar to that of DSA, without the latter's risks.

Recent studies, moreover, have indicated that CTA gives good results in the evaluation of other important plaque characteristics such as, for example, the presence of ulcerations and in the definition of plaque composition (fatty, mixed and calcified components). In particular, CTA, besides its ability to determine the degree of stenosis, correctly characterizes plaque morphology and plaque position. MRI noninvasively provides good results in the study of the carotid artery, and is probably the correct choice if the clinician seeks to characterize plaque composition, and determine whether intraplaque hemorrhage [93] or a fissured fibrous cap is present. However, MRI has several drawbacks compared to CTA, including longer examination times with resultant motion artifacts, pulsation artifacts, turbulent flow and in-plane flow, leading to exaggeration of the stenosis and poor demonstration of calcium.

Expected developments in the study of the carotid artery using CTA are about its capacity in the characterization of the plaque and some determinants of vulnerability such as the presence of a thin/thick fibrous cap, the presence of a fissured fibrous cap and correct identification of intraplaque hemorrhage.

An important potential drawback of this technique is the radiation dose. This is the major disadvantage in the use of CT. The radiologist has to understand the technical aspects in order to use it to obtain adequate diagnostic images while at the same time administering the lowest radiation dose possible.

References

1. Savory WS (1856) Case of a young woman in whom the main arteries of both upper extremities and of the left side of the neck were throughout completely obliterated. Med-Chir Trans Lond 39:205–219
2. Gibbs RG, Todd JC, Irvine C, Lawrenson R, Newson R, Greenhalgh RM, Davies AH (1998) Relationship between the regional and national incidence of transient ischemic attack and stroke and performance of carotid endarterectomy. Eur J Vasc Endovasc Surg 16:47–52
3. Adelman SM (1981) The National Survey of Stroke. Economic impact. Stroke 12(2 Pt 2 Suppl 1):I69–I87
4. Robins M, Baum HM (1981) National Survey of Stroke. Incidence. Stroke 12(2 Pt 2 Suppl 1):I45–I57
5. Grego F, Antonello M Lepidi S et al (2005) Is contralateral carotid artery occlusion a risk factor for carotid endarterectomy? Ann Vasc Surg 19:882–889

6. Fox AJ, Eliasziw M, Rothwell PM et al (2005) Identification, prognosis, and management of patients with carotid artery near occlusion. AJNR Am J Neuroradiol 26:2086–2094

7. Marcus HS, MacKinnon A (2005) Asymptomatic embolization detected by Doppler ultrasound predicts stroke risk in symptomatic carotid artery stenosis. Stroke 36:971–975

8. McCann RL (1994) Surgical management of carotid artery atherosclerotic disease. South Med J 86:S23–S28

9. North American Symptomatic Carotid Endarterectomy Trial Collaborators (1991) Beneficial effect of carotid endarterectomy in symptomatic patients high with grade stenosis. N Engl J Med 325:445–453

10. European Carotid Surgery Trialists' Collaborative Group (1998) Randomised trial of endarterectomy for recently symptomatic carotid stenosis: final results of the MRC European Carotid Surgery Trial (ECST). Lancet 351:1379–1387

11. Asymptomatic Carotid Atherosclerosis Group (1995) Endarterectomy for asymptomatic carotid artery stenosis. JAMA 273:1421–1428

12. Eliasziw M, Streifler JY, Fox AJ et al (1994) Significance of plaque ulceration in symptomatic patients with high-grade carotid stenosis: North American Symptomatic Carotid Endarterectomy Trial. Stroke 25:304–308

13. Naghavi M, Libby P, Falk E et al (2003) From vulnerable plaque to vulnerable patient: a call for new definitions and risk assessment strategies. Part I. Circulation 108:1664–1672

14. Ouhlous M, Flach HZ, de Weert TT et al (2005) Carotid plaque composition and cerebral infarction: MR imaging study. AJNR Am J Neuroradiol 26:1044–1049

15. Nandalur KR, Baskurt E, Hagspiel K, Phillips CD, Kramer CM (2005) Calcified carotid atherosclerotic plaque is associated less with ischemic symptoms than is noncalcified plaque on MDCT. AJR Am J Roentgenol 184:295–298

16. Mann JM, Davies MJ (1996) Vulnerable plaque. Relation of characteristics to degree of stenosis in human coronary arteries. Circulation 94:928–931

17. Wasserman BA, Wityk RJ, Trout HH, Virmani R (2005) Low-grade carotid stenosis: looking beyond the lumen with MRI. Stroke 36:2504–2513

18. Saba L, Caddeo G, Sanfilippo R, Montisci R, Mallarini G (2007) Efficacy and sensitivity of axial scans and different reconstruction methods in the study of the ulcerated carotid plaque using multidetector-row CT angiography: comparison with surgical results. AJNR Am J Neuroradiol 28:716–723

19. Rydberg J, Buckwalter KA, Caldemeyer KS et al (2000) Multisection CT: scanning techniques and clinical applications. Radiographics 20:1787–1806

20. Leclerc X, Godefroy O, Lucas C et al (1999) Internal carotid artery stenosis: CT angiography with volume rendering. Radiology 210:673–682

21. Yoon DY, Yun SY, Choi CS et al (2006) Multi-detector row CT of the head and neck: comparison of different volumes of contrast material with and without saline chaser. Neuroradiology 48:935–942

22. de Monye C, Cademartiri F, de Weert TT et al (2005) Sixteen-detector row CT angiography of carotid arteries: comparison of different volumes of contrast material with and without a bolus chaser. Radiology 237:555–562

23. Shetty Prashant G, Jhaveri KS (2000) Neurovascular applications of CT angiography. Indian J Radiol Imaging 10:211–220

24. Clave JL, Wise SW, Hopper KD et al (1997) Evaluation of contrast densities in the diagnosis of carotid stenosis by CT angiography. AJR Am J Roentgenol 169:569–573

25. Lell MM, Anders K, Uder M et al (2006) New techniques in CT angiography. Radiographics 26:S45–S62

26. Flohr T, Stierstorfer K, Bruder H, Simon J, Schaller S (2002) New technical developments in multislice CT–part 1: Approaching isotropic resolution with sub-millimeter 16-slice scanning. Rofo 174:839–845

27. Flohr TG, Schaller S, Stierstorfer K et al (2005) Multi-detector row CT systems and image-reconstruction techniques. Radiology 235:756–773

28. de Monye C, de Weert TT, Zaalberg W, Cademartiri F, Siepman DA, Dippel DW, van der Lugt A (2006) Optimization of CT angiography of the carotid artery with a 16-MDCT scanner: craniocaudal scan direction reduces contrast material-related perivenous artifacts. AJR Am J Roentgenol 186:1737–1745

29. Dix JE, Evans AJ, Kallmes DF, Sobel AH, Phillips CD (1997) Accuracy and precision of CT angiography in a model of carotid artery bifurcation stenosis. AJNR Am J Neuroradiol 18:409–415

30. Porsche C, Walker L, Mendelow D, Birchall D (2001) Evaluation of cross-sectional luminal morphology in carotid atherosclerotic disease by use of spiral CT angiography. Stroke 32:2511–2515

31. McKinney AM, Casey SO, Teksam M et al (2005) Carotid bifurcation calcium and correlation with percent stenosis of the internal carotid artery on CT angiography. Neuroradiology 47:1–9

32. Prokop M, Shin HO, Schanz A, Schaefer-Prokop C (1997) Use of maximum intensity projections in CT angiography: a basic review. Radiographics 17:433–451

33. Ertl-Wagner BB, Bruening R, Blume J, Hoffmann RT, Mueller-Schunk S, Snyder B, Reiser MF (2006) Relative value of sliding-thin-slab multiplanar reformations and sliding-thin-slab maximum intensity projections as reformatting techniques in multisection CT angiography of the cervicocranial vessels. AJNR Am J Neuroradiol 27:107–113

34. Cody DD (2002) AAPM/RSNA physics tutorial for residents: topics in CT. Image processing in CT. Radiographics 22:1255–1268

35. Napel S, Rubin GD, Jeffrey RB Jr (1993) STS-MIP: a new reconstruction technique for CT of the chest. J Comput Assist Tomogr 17:832–838

36. Rubin GD, Silverman SG (1995) Helical (spiral) CT of the retroperitoneum. Radiol Clin North Am 33:903–932

37. Rankin SC (1998) Spiral CT: vascular applications. Eur J Radiol 28:18–29

38. Rubin GD, Dake MD, Semba CP (1995) Current status of three-dimensional spiral CT scanning for imaging the vasculature. Radiol Clin North Am 33:51–70

39. Calhoun PS, Kuszyk BS, Heath DG, Carley JC, Fishman EK (1999) Three-dimensional volume rendering of spiral CT data: theory and method. Radiographics 19:745–764

40. Ota H, Takase K, Rikimaru H, Tsuboi M et al (2005) Quantitative vascular measurements in arterial occlusive disease. Radiographics 25:1141–1158

41. Cumming MJ, Morrow IA (1994) Carotid artery stenosis: a prospective comparison of CT angiography and conventional angiography. AJR Am J Roentgenol 163:517–523

42. Schwartz RB, Jones KM, Chernoff DM et al (1992) Common carotid artery bifurcation: evaluation with spiral CT. Radiology 185:513–519

43. Marks MP, Napel S, Jordan JE, Enzman DR (1993) Diagnosis of carotid artery disease: preliminary experience with maximum-intensity-spiral CT angiography. AJR Am J Roentgenol 160:1267–1271

44. Leclerc X, Godefroy O, Pruvo JP, Leys D (1995) Computed tomographic angiography for the evaluation of carotid artery stenosis. Stroke 26:1577–1581

45. Link J, Brossmann J, Grabener M, Mueller-Hulsbeck S, Steffens JC, Brinkmann G, Heller M (1996) Spiral CT angiography and selective digital subtraction angiography of internal carotid artery stenosis. AJNR Am J Neuroradiol 17:89–94

46. Cinat M, Lane CT, Pham H, Lee A, Wilson SE, Gordon I (1998) Helical CT angiography in the preoperative evaluation of carotid artery stenosis. J Vasc Surg 28:290–300

47. Seemann MD, Englmeier K, Schuhmann DR, Minx C, Furst H, Heuck A, Reiser MF (1999) Evaluation of the carotid and vertebral arteries: comparison of 3D SCTA and IA-DSA – work in progress. Eur Radiol 9:105–112

48. Verhoek G, Costello P, Khoo EW, Wu R, Kat E, Fitridge RA (1999) Carotid bifurcation CT angiography: assessment of interactive volume rendering. J Comput Assist Tomogr 23:590–596

49. Hirai T, Korogi Y, Ono K, Murata Y, Takahashi M, Suginohara K, Uemura S (2001) Maximum stenosis of extracranial internal carotid artery: effect of luminal morphology on stenosis measurement by using CT angiography and conventional DSA. Radiology 221:802–809

50. Bozzao A, Floris R, Pocek M, Fasoli F, Garaci FG, Simonetti G (2001) Non-invasive assessment of epiaortic vessels. Comparison of magnetic resonance angiography with gadolinium, spiral computerized tomography angiography, and digital angiography. Radiol Med 101:48–53

51. Sameshima T, Futami S, Morita Y, Yokogami K, Miyahara S, Sameshima Y, Goya T, Wakisaka S (1999) Clinical usefulness and problems with three-dimensional CT angiography for the evaluation of atherosclerotic stenosis of the carotid artery: comparison with conventional angiography, MRA and ultrasound sonography. Surg Neurol 51:300–309

52. Bartlett ES, Walters TD, Symons SP, Fox AJ (2006) Quantification of carotid stenosis on CT angiography. AJNR Am J Neuroradiol 27:13–19

53. Woodcock RJ Jr, Goldstein JH, Kallmes DF et al (1999) Angiographic correlation of CT calcification in the carotid siphon. AJNR Am J Neuroradiol 20:495–499

54. Bartlett ES, Walters TD, Symons SP, Fox AJ (2006) Diagnosing carotid stenosis near-occlusions by using CT angiography. AJNR Am J Neuroradiol 27:632–637

55. Castillo M, Wilson JD (1994) CT angiography of the common carotid artery bifurcation: comparison between two techniques and conventional angiography. Neuroradiology 36:602–604

56. Rothwell PM, Eliasziw M, Gutnikov SA et al (2003) Analysis of pooled data from the randomized controlled trials of endarterectomy for symptomatic carotid stenosis. Lancet 361:107–116

57. Morgenstern LB, Fox AJ, Sharpe B et al (1997) The risks and benefits of carotid endarterectomy in patients with near-occlusion of the carotid artery. Neurology 48:911–915

58. Rothwell PM, Warlow CP (2000) Low risk of ischemic stroke in patients with reduced internal carotid artery lumen diameter distal to severe symptomatic carotid stenosis: cerebral protection due to low poststenotic flow? Stroke 31:622–630

59. Chen CJ, Lee TH, Hsu HL et al (2004) Multi-slice CT angiography in diagnosing total versus near occlusions of the internal carotid artery: comparison with catheter angiography. Stroke 35:83–85

60. Eliasziw M, Rankin RN, Fox AJ et al (1995) Accuracy and prognostic consequences of ultrasonography in identifying severe carotid artery stenosis. Stroke 26:1747–1752

61. Dawson DL, Zierler RE, Strandness DE et al (1993) The role of duplex scanning and arteriography before carotid endarterectomy: a prospective study. J Vasc Surg 18:673–680

62. Polak JF, Kalina P, Donaldson MC et al (1993) Carotid endarterectomy: preoperative evaluation of candidates with combined Doppler sonography and MR angiography: work in progress. Radiology 186:333–338

63. Ricotta JJ, Holen J, Schenk E et al (1984) Is routine angiography necessary prior to carotid endarterectomy? J Vasc Surg 1:96–102

64. Goodson SF, Flanigan P, Bishara RA et al (1987) Can carotid duplex scanning supplant arteriography in patients with focal carotid territory symptoms? J Vasc Surg 5:551–557

65. Collins P, McKay I, Rajagoplan S et al (2005) Is carotid duplex scanning sufficient as the sole investigation prior to carotid endarterectomy? Br J Radiol 78:1034–1037

66. Nederkoorn PJ, Mali WPT, Eikelboom BC et al (2002) Preoperative diagnosis of carotid artery stenosis. Accuracy of non-invasive testing. Stroke 33:2003–2008

67. Yucel EK, Anderson CM, Edelman RR et al (1999) Magnetic resonance angiography. Update on applications for extracranial arteries. Circulation 100:2284–2301

68. Cloft HJ, Murphy KJ, Prince MR, Brunber JA (1996) 3D gadolinium-enhanced MR angiography of the carotid arteries. Magn Reson Imaging 14:593–600

69. Riedy G, Golay X, Melhem ER (2005) Three-dimensional isotropic contrast enhanced MR angiography of the carotid artery using sensitivity-encoding and random elliptic centric k-space filling: technique optimization. Neuroradiology 47:668–673

70. Keller PJ, Drayer BP, Fram EK et al (1989) MR angiography with two-dimensional acquisition and three-dimensional display. Work in progress. Radiology 173:527–532

71. Masaryk TJ, Modic MT, Ruggieri PM et al (1989) Three-dimensional (volume) gradient echo imaging of the carotid bifurcation: preliminary clinical experience. Radiology 171:801–806

72. Warlaw JM, Lewis SC, Collie DA, Sellar R (2002) Interobserver variability of magnetic resonance angiography in the diagnosis of carotid artery stenosis – effect of observer experience. Neuroradiology 44:126–132

73. Anderson CM, Saloner D, Tsuruda JS et al (1990) Artifacts in maximum-intensity-projection display of MR angiograms. AJR Am J Roentgenol 154:623–629

74. Magarelli N, Scarabino T, Simeone AL et al (1998) Carotid stenosis: a comparison between MR and spiral CT angiography. Neuroradiology 40:367–373

75. Nael K, Villablanca JP, Pope WB et al (2007) Supraaortic arteries: contrast enhanced MR angiography at 3.0 T – highly accelerated parallel acquisition for improved spatial resolution over an extended field of view. Radiology 42:600–609

76. Fayad ZA, Fuste V (2001) Clinical imaging of the high risk or vulnerable atherosclerotic plaque. Circ Res 89:305–316

77. Virmani R, Kolodgie FD, Burke AP et al (2000) Lessons from sudden coronary death: a comprehensive morphological classification scheme for atherosclerotic lesions. Arterioscler Thromb Vasc Biol 20:1262–1275

78. Newby AC, Libby P, van der Wal AC (1999) Plaque instability – the real challenge for atherosclerosis research in the next decade? Cardiovasc Res 41:321–322

79. de Weert TT, Ouhlous M, Meijering E et al (2006) In vivo characterization and quantification of atherosclerotic carotid plaque components with multidetector computed tomography and histopathological correlation. Arterioscler Thromb Vasc Biol 26:2366–2372

80. de Weert TT, Ouhlous M, Zondervan PE et al (2005) In vitro characterization of atherosclerotic carotid plaque with multidetector computed tomography and histopathological correlation. Eur Radiol 15:1906–1914

81. Schroeder S, Kopp AF, Baumbach A et al (2001) Non-invasive detection and evaluation of the atherosclerotic plaque with

multislice computed tomography. J Am Coll Cardiol 37:1430–1435

82. Gillard GH (2003) Imaging of the carotid artery disease: from luminology to function. Neuroradiology 45:671–680

83. Toussaint J-F, LaMuraglia GM, Southern JF, Fuster V, Kantor HL (1996) Magnetic resonance images lipid, fibrous, calcified, hemorrhagic, and thrombotic components of human atherosclerosis in vivo. Circulation 94:932–938

84. Shinnar M, Fallon JT, Wehrli S, Levin M, Dalmacy D, Fayad ZA, Badimon JJ, Harrington M, Harrington E, Fuster V (1999) The diagnostic accuracy of ex vivo MRI for human atherosclerotic plaque characterization. Arterioscler Thromb Vasc Biol 19:2756–2761

85. Hatsukami TS, Ross R, Polissar NL, Yuan C (2000) Visualization of fibrous cap thickness and rupture in human atherosclerotic plaque in vivo with high-resolution magnetic resonance imaging. Circulation 102:959–964

86. Coombs BD, Rapp JH, Ursell PC et al (2001) Structure of plaque at carotid bifurcation: high-resolution MRI with histological correlation. Stroke 32:2516–2521

87. Trivedi RA, U-King-IM JM, Graves MJ et al (2004) MRI-derived measurements of fibrous-cap and lipid core thickness: the potential for identifying vulnerable carotid plaques in vivo. Neuroradiology 46:738–743

88. Cai J, Hatsukami TS, Ferguson MS, Kerwin MS et al (2005) In vivo quantitative measurement of intact fibrous cap and lipid-rich necrotic core size in atherosclerotic carotid plaque: comparison of high resolution, contrast enhanced magnetic resonance imaging and histology. Circulation 112:3437–3444

89. Li ZY, Howarth S, Trivedi RA et al (2006) Stress analysis of carotid plaque rupture based on in vivo high resolution MRI. J Biomech 39:2611–2622

90. Li ZY, Howarth SP, Tang T et al (2007) Structural analysis and magnetic resonance imaging predict plaque vulnerability: a study comparing symptomatic and asymptomatic individuals. J Vasc Surg 45:768–775

91. Saloner D, Acevedo-Bolton G, Wintermark M, Rapp JH (2007) MRI of geometric and composition features of vulnerable carotid plaque. Stroke 38:637–641

92. Wexler L, Brundage B, Crouse J et al (1996) Coronary artery calcification: pathophysiology, epidemiology, imaging methods, and clinical implications – a statement for health professionals from the American Heart Association Writing Group. Circulation 94:1175–1192

93. Saam S, Cai J, Ma L et al (2006) Comparison of symptomatic and asymptomatic atherosclerotic carotid plaque features with in vivo MR imaging. Radiology 240:464–472

94. Saba L, Caddeo G, Sanfilippo R, Montisci R, Mallarini G (2006) Fissured fibrous cap and symptomaticity: are they correlated? Proceedings of the RSNA 2006 Annual Meeting. Radiological Society of North America, Oak Brook, IL, p 457

95. Yuan C, Zhang SX, Polissar NL et al (2002) Identification of fibrous cap rupture with magnetic resonance imaging is highly associated with recent transient ischemic attack or stroke. Circulation 105:181–185

96. Yuan C, Mitsumori LM, Beach KW, Maravilla KR (2001) Carotid atherosclerotic plaque: noninvasive MR characterization and identification of vulnerable lesions. Radiology 221:285–299

97. Cury RC, Houser SL, Furie KL et al (2006) Vulnerable plaque detection by 3.0 tesla magnetic resonance imaging. Invest Radiol 41:112–115

98. Takaya N, Yuan C, Chu B et al (2005) Presence of intraplaque hemorrhage stimulates progression of carotid atherosclerotic plaques. Circulation 111:2768–2775

99. Beach KW, Hatsukami T, Detmer PR (1993) Carotid artery intraplaque hemorrhage and stenting velocity. Stroke 24:314–319

100. Oliver TB, Lammie GA, Wright AR et al (1999) Atherosclerotic plaque at the carotid bifurcation: CT angiographic appearance with histopathologic correlation. AJNR Am J Neuroradiol 20:897–901

101. Culebras A, Magana R, Cacayorin ED (1988) Computed tomography of the cervical carotid artery: significant of the lucent defect. Stroke 19:723–727

102. Randoux B, Marro B, Koskas F et al (2001) Carotid artery stenosis: prospective comparison of CT, three-dimensional gadolinium-enhanced MR, and conventional angiography. Radiology 220:179–185

103. Runge VM, Kirsch JE, Lee C (1993) Contrast-enhanced MR angiography. J Magn Reson Imaging 3:233–239

104. Saba L, Caddeo G, Sanfilippo R, Montisci R, Mallarini G (2007) CT and US in the study of ulcerated carotid plaque compared with surgical results. Advantages of multi-detector-row CT angiography. AJNR Am J Neuroradiol 28:1061–1066

105. Debernardi S, Martincich L, Lazzaro D et al (2004) CT angiography in the assessment of carotid atherosclerotic disease: results of more than two years' experience. Radiol Med 108:116–127

106. Lammie GA, Wardlaw J, Allan P, Ruckley CV, Peek R, Signorini DF (2000) What pathological components indicate carotid atheroma activity and can these be identified reliably using ultrasound? Eur J Ultrasound 11:77–86

107. Bluth EI, McVay LV, Merritt CR, Sullivan A (1998) The identification of ulcerative plaque with high resolution duplex carotid scanning. J Ultrasound Med 7:73–76

108. Alvarez-Linera J, Benito-Leon J, Escribano J, Campollo J, Gesto R (2003) Prospective evaluation of carotid artery stenosis: elliptic centric contrast-enhanced MR angiography and spiral CT angiography compared with digital subtraction angiography. AJNR Am J Neuroradiol 24:1012–1019

109. Lays D, Malin T, Stojkovic T et al (1995) Follow up of patients with history of carotid artery dissection. Cerebrovasc Dis 5:43–49

110. Leclerc X, Godefroy O, Salhi A et al (1998) Helical CT for the diagnosis of extracranial carotid artery dissections. AJNR Am J Neuroradiol 19:831–837

111. Rothwelll PM, Gibson R, Warlow CP (2000) Interrelation between plaque surface morphology and degree of stenosis on carotid angiograms and the risk of ischemic stroke in patients with symptomatic carotid stenosis. Stroke 31:615–621

112. Malek AM, Alper SL, Izumo S (1999) Hemodynamic shear stress and its role in atherosclerosis. JAMA 282:2035–2042

113. Hennerici M, Rautenberg W, Mohr S (1982) Stroke risk from symptomless extracranial arterial disease. Lancet 2:1180–1183

114. Barnett HJ, Taylor DW, Eliasziw M, Fox AJ, Ferguson GG, Haynes RB, Rankin RN, Clagett GP, Hachinski VC, Sackett DL, Thorpe KE, Meldrum HE; for the North American Symptomatic Carotid Endarterectomy Trial Collaborators (1998) Benefit of carotid endarterectomy in patients with symptomatic moderate or severe stenosis. N Engl J Med 339:1415–1425

115. Sitzer M, Puac D, Buehler A et al (2003) Internal carotid artery origin. A novel risk factor for atherosclerosis. Stroke 39:950–955

116. Schulz UG, Rothwell PM (2001) Sex differences in carotid plaque bifurcation anatomy and the distribution of atherosclerotic plaque. Stroke 32:1525–1531

117. Adams GJ, Simoni DM, Bordelon CB et al (2002) Bilateral symmetry of human carotid artery atherosclerosis. Stroke 33:2575–2580

118. Gnasso A, Irace C, Carallo C et al (1997) In vivo association between low wall shear stress and plaque in subjects with asymmetrical carotid atherosclerosis. Stroke 28:993–998

119. Rouleau PA, Huston J, Gilbertson J, Brown RD Jr, Meyer FB, Bower TC (1999) Carotid artery tandem lesions: frequency of angiographic detection and consequences for endarterectomy. AJNR Am J Neuroradiol 20:621–625

120. Skutta B, Fürst G, Eilers J et al (1999) Intracranial steno-occlusive disease: double-detector helical CT angiography versus digital subtraction angiography. AJNR Am J Neuroradiol 20:791–799

121. Lasser EC (1987) A coherent biochemical basis for increased reactivity to contrast material in allergic patients: a novel concept. AJR Am J Roentgenol 149:1281–1285

122. Cochran ST, Bomyea K, Sayre JW (2001) Trends in adverse events after IV administration of contrast media. AJR Am J Roentgenol 176:1385–1388

123. Cohan RH, Bullard MA, Ellis JH et al (1997) Local reactions after injection of iodinated contrast material: detection, management and outcome. Acad Radiol 4:711–718

124. Cashaman JD, McCredie J, Henry DA (1991) Intravenous contrast media: use and associated mortality. Med J Aust 155:618–623

125. Morcos SK (2005) Acute serious and fatal reactions to contrast media: our current understanding. Br J Radiol 78:686–693

126. Gleeson TG, Bulugahapitiya S (2004) Contrast induced nephropathy. AJR Am J Roentgenol 183:1673–1689

127. Murphy SW, Barrett BJ, Parfrey PS (2000) Contrast nephropathy. J Am Soc Nephrol 11:177–182

128. Cinat ME, Pham H, Vo D et al (1999) Improved imaging of carotid artery bifurcation using helical computed tomographic angiography. Ann Vasc Surg 13:178–183

129. Nickoloff E, Alderson P (2001) Radiation exposure to patients from CT: reality, public perception, and policy. AJR Am J Roentgenol 177:285–287

130. Ertl-Wagner BB, Hoffmann RT, Bruning R, Herrmann K, Snyder B, Blume JD, Reiser MF (2004) Multi-detector row CT angiography of the brain at various kilovoltage settings. Radiology 231:528–535

131. Ertl-Wagenr B, Hoffmann RT, Bruning R et al (2002) Diagnostic Evaluation of the craniocervical vascular system with 16-slice multi-detector row spiral CT. Protocols and first experience (in German). Radiologe 42:728–732

132. Clevert DA, Johnson T, Jung EM et al (2006) Color doppler, power doppler and B-flow ultrasound in the assessment of ICA stenosis: comparison with 64-MD-CT angiography. Eur Radiol. DOI 10.1007/s00330-006-0488-7

133. Kalra MK, Maher MM, Kamath RS et al (2004) Sixteen-detector row CT of abdomen and pelvis: study for optimization of Z-axis modulation technique performed in 153 patients. Radiology 233:241–249

134. Kalra MK, Maher MM, Kamath RS et al (2004) Comparison of z-axis automatic tube current modulation technology with fixed tube current CT scanning of abdomen and pelvis. Radiology 232:347–353